

Chapter 17

Numerical Simulation of Turbulent Combustion in Internal Combustion Engines

Xue-Song Bai

Abstract The combustion process in internal combustion engines can occur in multiple modes. In spark-ignition (SI) engines it is mainly a turbulent premixed flame propagation process; however, since the charge is at elevated temperature and pressure, it is possible to have autoignition in the unburned charge, which can lead to engine knock. In conventional Diesel engines, the combustion process is first started with the onset of ignition and followed by turbulent diffusion flames. In the development of modern compression ignition engines, the tendency is to use a mixed mode combustion in order to reduce soot and NO_x emissions. Examples of such engine concepts are homogeneous charge compression ignition (HCCI), reactivity controlled compression ignition (RCCI), and partially premixed combustion (PPC) engines. To meet the challenge of high-performance numerical simulations in today's engine design it is necessary that the simulation models shall handle the different modes of combustion. In this chapter, the various combustion modes will be reviewed. Recent simulation results that reveal the finely detailed reaction zone structures in HCCI, RCCI, and PPC engines will be discussed. The challenges in the modeling of multiple modes combustion in internal combustion engine will be discussed in the frameworks of large-eddy simulation and Reynolds-averaged Navier–Stokes simulations. Finally, state-of-the-art models for the various combustion modes will be reviewed, focusing on the modeling of multimodes combustion problems.

Keywords Internal combustion engine • Homogeneous charge compression ignition • Partially premixed combustion • Low temperature combustion
Numerical simulation

X.-S. Bai (✉)

Division of Fluid Mechanics, Department of Energy Sciences, Lund University,
221 00 Lund, Sweden
e-mail: Xue-Song.Bai@energy.lth.se

© Springer Nature Singapore Pte Ltd. 2018
S. De et al. (eds.), *Modeling and Simulation of Turbulent Combustion*, Energy,
Environment, and Sustainability, https://doi.org/10.1007/978-981-10-7410-3_17

513

17.1 Introduction

Numerical simulation using Computational Fluid Dynamics (CFD) methods is widely used today to study in-cylinder flow and combustion process in internal combustion engines (ICE). Depending on the purpose of the simulations one can find different types of numerical simulations. One type of numerical simulation is aimed at gaining insight into the turbulent combustion physics in ICE; to do this, the numerical simulations are usually based on the so-called direct numerical simulation (DNS) approach. In DNS, the full set of transport equations is solved numerically using high-order accuracy numerical methods, considering molecular transport properties and relatively detailed chemical kinetic mechanisms (Chen 2011; Sankaran et al. 2005). DNS resolves all physical and chemical scales in the engine combustion process, which is computationally prohibitive at the moment. In a recent DNS of partially premixed combustion (PPC) of a n-heptane/iso-octane/air mixture in a $0.6 \times 0.6 \times 0.6$ mm constant volume domain, with 512^3 computational cells, 3.5 millions of CPU hours were required to simulate the combustion process of physical time about 0.26 ms (about 1.7 times of the integral time) (Zhang et al. 2015a), using the CURIE TN computer based in France at the Tres Grand Centre de Calcul (TGCC). Although DNS is not feasible for numerical simulations of multiple-cycle ICE combustion process with real engine geometry, it is powerful in exploring the fundamental details of ICE combustion process and outstanding findings have been obtained in recent years that can help understanding of the reaction zone structures of ICE combustion and guiding the development of simplified combustion models used for numerical simulations of practical engines.

The second type numerical simulations are aimed at studying the real engine combustion process for the development of new ICE. Today's ICE development is driven by the demands on the emission compliance, CO₂ emissions, performance, and cost-effectiveness, which has affected the development process of the combustion system in ICE industry. As an example, Persson et al. recently demonstrated a new design process (Persson et al. 2017), in which numerical simulations were heavily used in the development of the next-generation Volvo Cars diesel combustion system that was aimed at complying with Euro 6d including Real Driving Emissions (RDE). First, the requirements for the system were determined, after which key factors that affected the system performance were selected, such as the charge motion, combustion chamber geometry, and injector nozzle geometry. Based on the requirements, a robust charge motion with desired flow characteristics was defined. Numerical simulations were performed to optimize the combustion chamber geometry and spray system. The selected solutions were then verified by creating rapid prototype pistons for evaluation. With the aid of numerical simulations, the number of development loops for the engine can be reduced, resulting in a reduction of development cost and time.

To apply numerical simulations to ICE design the computation must be both reasonably accurate and computationally affordable. To do this, one has to rely on methods that employ certain averages or spatial filtering, through which the small-scales

of flow and reaction zone structures are removed, leaving the mean flow or large-scale flow motion and combustion phenomenon described by the governing equations to be resolved by coarse grid resolution. The well-known Reynolds-averaged Navier–Stokes (RANS) method is based on ensemble or time averages, whereas large-eddy simulation (LES) is based on the spatial filtering. RANS is used today in industrial engine design (Ge et al. 2010; Persson et al. 2017) due to its computational low cost; however, only the mean flow is simulated in RANS, while in many situations, large-scale unsteady turbulence structure is also of concern, e.g., when studying cyclic variation of ICE. In LES, the large-scale turbulent motion is simulated while only scales smaller than the spatial filter size are filtered away. Since the detailed turbulence structures in RANS and partly in LES are not simulated, the effect of small-scale turbulence structures on the mean or large-scale turbulence motion is included in the correlation terms in the RANS and LES governing equations. These terms need to be modeled to close the governing equations. The results of RANS and LES are essentially dictated by these models.

17.2 Challenges in Modeling of Turbulent Combustion in ICE

To describe the problem we consider the governing equations for RANS and LES. In general, the in-cylinder flow in ICE is at low Mach numbers during the compression and combustion strokes, after the intake valves are closed. Due to the piston motion, the flow is compressible and the thermodynamic conditions are transient. In ICE even the mean flow is unsteady: the piston is continuously reciprocating, which drives the flow to compress or expand. The Reynolds number is high thus the flow is turbulent. When the fuel is directly injected into the cylinder the problem involves liquid/gas two-phase flow. When the fuel/air mixture is ignited chemical reactions occur in the mixture, which often involves a large number of chemical species and elementary reactions.

In RANS, the mean flow can be computed by introducing cycle averages (also known as ensemble or phase averages), viz.,

$$\overline{Q}(\mathbf{x}, t) = \frac{1}{N_c} \sum_i^{N_c} Q_i(\mathbf{x}, t), \quad (17.1)$$

where $Q(\mathbf{x}, t)$ is a quantity describing the flow motion (e.g., velocity component) or thermodynamic property (e.g., density, temperature, or pressure) at point \mathbf{x} and time t . N_c is the number of cycles used in the cycle average, and subscript i denotes the i th cycle. A quantity with overbar denotes the cycle averaged quantity. When applying cycle averages to the experimental data the cyclic variation of the mean flow is lumped into the turbulent fluctuation part (Heywood 1988), while in RANS the cyclic variation of the mean flow is not accounted.

In LES the governing equations are spatially filtered. The spatial filtering of a quantity $Q(\mathbf{y}, t)$ is defined as its convolution with a filter function, $G(\mathbf{y}; \Delta)$, viz.,

$$\bar{Q}(\mathbf{x}, t) = \int_{\Omega} Q(\mathbf{y}, t) G(\mathbf{x} - \mathbf{y}; \Delta(\mathbf{x})) d\mathbf{y}, \quad (17.2)$$

where the integration is defined over the entire flow domain Ω . Δ is the characteristic length of the spatial filter, which, in general, may vary with position. Here, the quantity with overbar denotes the spatial filtered quantity. Since the spatial filtering is local and based on the single cycle, cyclic variations of the mean flow are retained in the LES solution. Several authors have demonstrated the capability of using LES to study cyclic variations in spark-ignition (SI) engines (Haworth 1999; Vermorel et al. 2009). When using LES to simulate the cycle averaged mean flows the computational effort is rather high, since many cycles, e.g., at least 10 cycles, have to be simulated to obtain a reasonably converged mean field (Vermorel et al. 2009).

For reacting flows density weighted ensemble average or spatial filtering is used, i.e., $\tilde{Q}(\mathbf{x}, t) = \bar{\rho}\tilde{Q}/\bar{\rho}$, where ρ is the density of the local mixture, and the quantity with an over-tilde denotes the density weighted ensemble averaged or filtered quantity. Applying the density weighted ensemble average or spatial filtering to the governing equations of turbulent reactive flows results in the following averaged or filtered equation for RANS or LES, e.g., for the transport equation of species mass fraction, Y_k ,

$$\frac{\partial \bar{\rho}\tilde{Y}_k}{\partial t} + \frac{\partial \bar{\rho}\tilde{u}_i\tilde{Y}_k}{\partial x_i} = \frac{\partial}{\partial x_i} \left(\bar{\rho}\tilde{u}_i\tilde{Y}_k - \overline{\rho u_i Y_k} - \frac{\partial \bar{J}_{k,i}}{\partial x_i} \right) + \bar{\rho}\tilde{\omega}_k, \quad (17.3)$$

where u_i is the velocity component along the Cartesian coordinate x_i direction, $J_{k,i}$ is the molecular transport flux of species k along x_i direction, and ω_k is the net formation rate of species k due to chemical reactions.

Although Eq. (17.3) in RANS and LES has the same form the quantities and terms in the equation have completely different physical meaning. In RANS, the turbulent scalar fluxes $(\bar{\rho}\tilde{u}_i\tilde{Y}_k - \overline{\rho u_i Y_k})$ and mean reaction rates $\tilde{\omega}_k$ are from the contribution of the entire turbulence spectrum, while in LES the large-eddy motion is described by the filtered quantities $(\bar{\rho}, \tilde{u}_i, \tilde{Y}_k)$ from the filtered governing equations, in which the effect of small sub-grid scale (SGS) motion is taken into account in the sub-grid scalar transport flux $(\bar{\rho}\tilde{u}_i\tilde{Y}_k - \overline{\rho u_i Y_k})$ and the spatially filtered chemical reaction rate $\tilde{\omega}_k$. In RANS the turbulent scalar fluxes and mean reaction rate are independent of the grid cell size used in numerical simulations, while in LES the SGS scalar fluxes and the filtered reaction rate are not independent of the grid cell size. Since the filter size is proportional to the cell size, in LES when the filter size (cell size) decreases to the level that all flow and chemical reaction layer scales are resolved, the SGS scalar fluxes vanish and the filtered reaction rate is that of the unfiltered one; LES then becomes DNS.

The challenge in the modeling of turbulent combustion lies in the modeling of these turbulent transport fluxes and the averaged reaction rates. In RANS, various

models have been developed for the turbulent transport fluxes (and Reynolds stresses in the mean momentum equations). Very often two-equation $k - \epsilon$ models are used in ICE flow and combustion simulations (Reitz and Rutland 1995). In LES of ICE, a number of authors have modeled the sub-grid scalar fluxes and the sub-grid stresses (for the momentum equations) using the Smagorinsky model (Smagorinsky 1963), viz., for the scalar fluxes,

$$\overline{\rho \tilde{u}_i \tilde{Y}_k} - \overline{\rho u_i \tilde{Y}_k} = \frac{\mu_{SGS}}{\sigma_{SGS}} \frac{\partial \tilde{Y}_k}{\partial x_i}, \quad (17.4)$$

where the sub-grid diffusion coefficient μ_{SGS} is modeled as $\mu_{SGS} = \overline{\rho} (C_s \Delta)^2 |\tilde{S}_{ij}|$, with \tilde{S}_{ij} being the mean strain rate tensor and $|\tilde{S}_{ij}| = \sqrt{2\tilde{S}_{ij}\tilde{S}_{ij}}$. σ_{SGS} is the turbulent Schmidt/Prandtl number typically assigned the value of 1. The Smagorinsky constant C_s is often set a value of 0.17, which may, however, be different in different flow problems. This model constant can be determined dynamically by employing two different filtering operations, using a method known as the dynamic Smagorinsky model (Germano et al. 1991). A more complete review on the various SGS models used in ICE simulations has been given by Rutland (2011).

The mean reaction rate or the filtered reaction rate $\tilde{\omega}_k$ is the main challenge to model in RANS or LES. The combustion process is very different in different types of ICE, thus, specialized models for different types of engines have been developed. For example, for Diesel engines flamelet models based on the mixture fraction and scalar dissipation rate have been developed and widely used in engine combustion simulations (Felsch et al. 2007; Hasse et al. 1999; Mittal et al. 2012; Pitsch et al. 1996), whereas for spark-ignition engines, one can find ICE simulations using the coherent flame model (Marble and Broadwell 1977) based on a transport equation for flame surface density (Candel and Poinso 1990), and level-set G-equations models (Peters 2000). Certainly, a longer list of specialized models exists and some of them will be discussed later in this chapter. A more comprehensive review on various models can be found in Reitz and Rutland (1995); Rutland (2011). These specialized models are valid for the combustion process for which the models were developed, while application of these specialized models to other types of combustion problems is often not acceptable. The idea of developing a specialized model for certain types of engines is to remove some of the unimportant physics details in the modeling to achieve the best efficiency of the simulation while retaining an acceptable accuracy of the simulation results.

From the model robustness point of view, a generalized model that is valid for multimodes combustion is most preferable, although such a model is often computationally expensive. General models are based on finite-rate chemistry coupling with the flow simulations, with the mean reaction rate or the filtered reaction rate $\tilde{\omega}_k$ explicitly modeled. Examples of models for $\tilde{\omega}_k$ are the partially stirred reactor model (PaSR), the eddy dissipation concept (EDC) model (Magnussen and Hjertager 1977), the effective time-scale model (Kong et al. 1995), and the transported probability density (PDF) models (Pope 1985), among others. Transported PDF models

have the advantage of directly closing the mean reaction rate terms, although the effect of molecular mixing on the evolution of the PDF requires further modeling. A challenge in the PDF models is the reduction of computational time and speedup of the computation.

In the remaining sections of this chapter, some specialized models for SI engines and Diesel engines will be reviewed briefly, followed by a presentation of the recent numerical simulations of low-temperature combustion engines, where multiple combustion modes exist and thus general models are often required to simulate these ICE combustion processes.

17.3 Numerical Simulation of Turbulent Combustion in Spark-Ignition Engines and Conventional Diesel Engines

Conventional SI engines and Diesel engines are the two types of engines dominating the market. Numerical simulations of the combustion process in these engines have a long history and successful experience, as demonstrated in the recent work of Persson et al. (2017). Extensive reviews on the numerical simulations and CFD models for SI engines and Diesel engines can be found in the literature, e.g., Reitz and Rutland (1995); Rutland (2011). In this section, a brief review on the CFD models often used in SI and Diesel engines is presented, aiming at bridging the discussion on the modeling of modern low-temperature combustion engines in Sect. 17.4.

17.3.1 Modeling of Turbulent Combustion in SI Engines

In spark-ignition (SI) engines the fuel is well mixed with the air before the initiation of combustion using a spark. The combustion process is mainly in the premixed flame mode. A premixed flame is characterized by the thin reaction layer that propagates into the unburned fuel/oxidizer mixture at a specific flame speed. In the reaction layer, the chemical reactions are initiated due to the heat and mass transfer from the burned hot products to the unburned colder mixture. The propagation speed of the reaction layer is, therefore, governed by both the molecular diffusion, turbulent transport, and chemical reactions. The essential key of modeling SI engine combustion is the modeling of the turbulent flame propagation speed in the engine. A large number of models have been developed for SI engine combustion simulations.

In SI engines, the propagation of turbulent premixed flames is at a high pressure and high temperature condition due to the piston compression. The thickness of the reaction zone becomes thinner with increasing compression ratio, while the laminar flame speed becomes larger with increasing compression ratio. The Kolmogorov micro length scale decreases with increasing compression ratio. The ratio

between the chemical time and the Kolmogorov time, known as the Karlovitz number, becomes smaller with increasing compression ratio,

$$Ka \sim Ka_0 r_c^{-2}, \quad (17.5)$$

where Ka_0 is the Karlovitz number at atmospheric condition (before compression) and Ka is the Karlovitz number during the combustion stroke near the top-dead-center (TDC). r_c is the compression ratio. In SI engines due to the high compression ratio the Karlovitz number is about 100 times smaller than that in atmospheric condition with the same turbulent large-eddy velocity and length scales. Thus, combustion processes in SI engines occur typically in low Karlovitz number combustion regimes, namely, the flamelet regimes and the thin reaction zones regime. The fundamental reaction zone structures in these regimes are similar to that of laminar flamelets (Peters 2000). The reaction zone in flamelet and thin-reaction zones regimes is not resolved in RANS and LES, which is in fact often treated as an interface separating the burned hot product and the unburned fuel/air mixture, e.g., in the well-known model of Bray–Libby–Moss (BML) (Bray et al. 1985). The thermochemical state across the flame is characterized using a reaction progress variable, defined as the normalized temperature, or mass fraction of the reactants or products. A governing equation for the mean progress variable (\bar{c}) is derived from the temperature or species transport equation,

$$\frac{\partial \bar{\rho} \bar{c}}{\partial t} + \frac{\partial \bar{\rho} \tilde{u}_i \bar{c}}{\partial x_i} = \frac{\partial}{\partial x_i} \left(\frac{\mu_t}{\sigma_t} \frac{\partial \bar{c}}{\partial x_i} \right) + \bar{\rho} \tilde{\omega}_c, \quad (17.6)$$

where μ_t is turbulent eddy viscosity in RANS and SGS viscosity in LES. σ_t is the turbulent Schmidt number, which is on the order of unity. The mean reaction rate for the progress variable $\tilde{\omega}_c$ is modeled in different ways in different models. In the BML model, $\tilde{\omega}_c$ is modeled by employing a presumed PDF for the progress variable. A recent development in this framework is described in Dunstan et al. (2013), where modeling of the the scalar dissipation rate of the reaction progress variable is discussed and the mean reaction rate can be modeled using the scalar dissipation rate.

The coherent flame model (CFM) is based on the flame surface density (FSD) concept. The model was originally proposed by Marble and Broadwell for modeling turbulent diffusion flames (Marble and Broadwell 1977), and it later became popular for modeling of turbulent premixed flames, both in the RANS and LES frameworks. A transport equation for FSD was postulated in the earlier work of Marble and Broadwell (1977), while a more rigid derivation of the model was given later (Candel and Poinso 1990; Pope 1988). The CFM model is also based on the assumption of flamelet combustion. In this model, the mean reaction rate is modeled to be proportional to FSD. A more recent development of this model is, for example, the extended coherent flame model (ECFM) of Colin et al. (2004) accounting for non-premixed flames, where in order to adapt the model to unmixed combustion for Diesel engine

application, a description of the mixing state had been added. It was represented by three mixing zones: a pure fuel zone, an air zone with possible residual gases, and a mixed zone in which the ECFM combustion model was applied. A mixing model was presented which allowed progressive mixing of the initially unmixed fuel and air.

Two models for SI flames that were developed based on the special treatment of the reaction zones are the thickened flame model (Colin et al. 2000) and the flamelet generated manifolds (FGM) (van Oijen et al. 2016). In the thickened flame model, the thin flamelet is numerically thickened by decreasing the reaction rates to allow for numerical resolution of the reaction layer. The numerical thickening is compensated by adjusting the diffusive transport terms to maintain the same laminar flame speed. The FGM model describes the flame front in a flame-adapted coordinate system, taking into account the effects of flame stretch in turbulent flames by resolving the detailed structure of flame stretch and curvature inside the flame front (van Oijen et al. 2016).

Another type of flamelet model for SI engine simulations is based on the level-set approach, e.g., the G-equation model (Peters 2000; Tan and Reitz 2006). In this model, the flame front is modeled as a thin layer propagation in the turbulent flow. The propagation of the reaction layer is modeled as a level-set function (G), whereas the local flame structure is expressed as a function of G . The mean flame quantities are calculated as an ensemble averages of premixed flamelets, through the G -function, see, e.g., Nilsson and Bai (2000). In the G-equation model, the level-set function G is usually converted to a distance function through a re-initialization procedure. The G-equation model has been applied to various flames, including flames with equivalence ratio stratification and local extinction (Carlsson et al. 2015; Nogenmyr et al. 2009). Tan and Reitz demonstrated the application of a G-equation model to SI engine simulations (Tan and Reitz 2006). They showed that the in-cylinder pressures and engine-out NO_x emissions could be well replicated, in comparison with the experiments, at various ignition timing conditions.

Due to the elevated temperature and pressure environment in the engine cylinder, the flame propagation in SI engines can be complex, for example, the unburned mixture in front of the flames can be partially reactive (Martz et al. 2011; Pan et al. 2016), which results in an elevated flame speed, depending on the fuels. The propagation of premixed flames in SI engines can eventually trigger the onset of autoignition in the unburned fuel/air mixture, which can lead to engine knock. Owing to the inhomogeneity in the unburned charge, typically existing either in the species composition or in temperature, the ignition process appears as thin spontaneous ignition fronts propagating at a speed that can be much higher than the flame speed. At the ignition front, the initiation of the reactions is not due to transport of heat and mass from the hot combustion products, but rather it is due to the high initial temperature and pressure in the mixture that gives rise to autoignition of the mixture. The propagation speed of the reaction front is inversely proportional to the gradient of the ignition delay time in the mixture (Zeldovich 1980). For ideally homogeneous mixture, the propagation speed of the ignition front is infinity.

In order to model the ignition process finite-rate chemistry is required. Since the reactions occur simultaneously in the unburned mixture, not just in a thin layer, the filtered reaction rates are less sensitive to the filter size and grid cell size. A simple well-stirred reactor model (WSR), in which the spatial variations of the thermodynamic properties in the sub-grid scale are neglected, can be sufficient to model the mean rates. The challenge is however in how to reduce the computational burden required when using a full set of transport equations and large chemical kinetic mechanisms needed for complex fuels. Several authors have developed tabulation approaches to couple the ignition chemistry in CFD simulations (Joelsson et al. 2012; Knop et al. 2011; Lecocq et al. 2011). In these models, the mean source term in Eq. (17.6) is computed through lookup tables based on the ignition calculation in homogenous mixture with detailed chemical kinetic mechanisms.

17.3.2 Modeling of Turbulent Combustion in Diesel Engines

Conventional compression-ignition engines are known as Diesel engines. The flow physics is complex due to the direct injection of liquid fuels that undergo atomization, evaporation, and turbulent mixing before the combustion process. Modeling of spray atomization, breakup, and evaporation processes is crucially important for the predictive simulation of turbulent combustion in Diesel engines, and comprehensive models have been developed and applied in diesel engine combustion simulations, cf. e.g., Reitz (1987) and Reitz and Rutland (1995), and references therein.

The combustion process in Diesel engines contains multiple combustion modes (Dec 1997). When the fuel is injected through a nozzle to the engine cylinder, the fuel is atomized and vaporized in the proximity of the nozzle by interacting with the hot ambient air. Thereafter, the fuel vapor and air mixture is ignited at a location downstream the fuel jet. A diffusion flame is then established and stabilized downstream the fuel nozzle. The distance between the leading front of the flame and the fuel nozzle is known as the liftoff length. Soot emission is known to be closely correlated with the liftoff length, see, e.g., Jangi et al. (2013). A longer liftoff length gives rise to a more sufficient mixing of the ambient air to the center fuel jet, which can lower the equivalence ratio in front of the flame, and thus, the soot formation can be reduced. It is therefore important to properly capture the liftoff phenomenon in numerical simulations of Diesel engine combustion.

Depending on the ambient temperature, two mechanisms, autoignition and flame propagation coupled with the low-temperature ignition, can be used to explain the liftoff position and stabilization of diesel flames (Gong et al. 2014). When the ambient temperature is low, the liftoff position is an autoignition induced flame-front (AIIF); the flame is stabilized as a two-stage autoignition process. When the ambient temperature is high, the liftoff position shows a structure similar to the classic triple-flame with the low-temperature ignition upstream; hence, the flame is stabilized by the triple flame propagation coupled with the low-temperature ignition (Gong et al. 2014).

To capture the leading flame front position one may use a general model based on the finite-rate chemistry model, since the low-temperature chemistry in the region in front of the leading flame front needs to be captured. When using finite-rate chemistry the mean reaction rate requires a model. Some authors have used the simple WSR model. A more general approach is to use the transported PDF model to account for the interaction between turbulence and chemical reactions. A comprehensive review of the transported PDF model can be found in the review paper by Haworth (2010).

Finite-rate chemistry-based models are computationally time consuming. They have been used in exploring the fundamental diesel flame physics in constant volume combustion vessels (Jangi et al. 2013; Gong et al. 2014) and in experimental optical engine studies (Solsjo et al. 2013), while it is too time consuming to use in engine design simulations in industry. Specialized models are developed for Diesel engine combustion simulations. Two examples of these models are the representative interactive flamelet (RIF) model (Felsch et al. 2007; Hasse et al. 1999; Pitsch et al. 1996) and the conditional moment closure (CMC) model (Klimenko and Bilger 1999; Mastorakos and Bilger 1998; Swaminathan and Bilger 1999).

In the RIF model, a reactive scalar is assumed to be a function of mixture fraction. This model implies that the flame is affected by turbulence through its transport of mixture fraction, while the flame structure in the mixture fraction coordinate is essentially similar under different turbulent flow conditions. Turbulence can affect the flamelet structure through the mixing rate. A set of unsteady flamelet equations is derived from the transport equations of species mass fractions and energy, with mixture fraction as the independent variable and scalar dissipation rate at stoichiometric mixture fraction as an input parameter that represents the mixing rate in the equations. The set of flamelet equations is solved interactively with the flow equations; important flow field information, such as thermodynamic pressure, scalar dissipation rate, and density, is exchanged with the flow simulations at every time step. The autoignition, combustion, and pollutant formation are all taken into account within a single RIF approach based on the detailed chemical kinetics. A recent evaluation of the RIF model and the finite-rate chemistry model with local well-stirred reactor, WSR, assumption within each CFD cell for diesel spray flames showed that, the RIF model and finite-rate chemistry model with WSR predicted the same ignition delay time, while the RIF model showed better capability in predicting the liftoff length than the well-stirred reactor model did (D'Errico et al. 2014).

In the CMC model, a set of governing equations is derived for the conditionally averaged quantities, e.g., species mass fractions conditioned on mixture fraction. Temporal and spatial variation of unconditionally averaged quantities can be obtained by integrating conditionally averaged values over the range of conserved scalar values after weighting with the local probability density function of the conserved scalar (Swaminathan and Bilger 1999). The CMC equations contain similar terms to that in the RIF equations, e.g., the diffusion term in the mixture fraction space with scalar dissipation rate as an input parameter. The CMC equations involve in addition an explicit term accounting for the convective fluxes in physical space.

This term disappears in homogeneous turbulence, thus, the resulting CMC equations are in a similar form to those of RIF (Swaminathan and Bilger 1999). The CMC model has been used to simulate spray autoignition (KIm and Huh 2002) and Diesel engine combustion with success (De Paola et al. 2008).

17.4 Numerical Simulation of Turbulent Combustion in LTC Engines

Low-temperature combustion (LTC) engine is a modern engine concept that was developed to comply with emission legislation and to improve the engine efficiency. Examples of such engine concept are homogeneous charge compression ignition (HCCI) (Najt and Foster 1983; Onishi et al. 1979), reactivity controlled compression ignition (RCCI) (Reitz and Ganesh 2015), and partially premixed combustion (PPC) engines (Kalghatgi et al. 2007; Manente et al. 2009). RCCI engine makes use of two different fuels with different reactivities, for example, gasoline (high octane number fuel, less easy to autoignite) and diesel (much easier to autoignite), to control the ignition timing and the heat release rate profiles to achieve optimal engine performance. Similar to Diesel engines, HCCI, and PPC are relying on a single fuel. The difference in these different engines is mainly in the injection timing of the fuel. In a Diesel engine, the fuel is injected late during the compression stroke near TDC to make use of the high pressure and high temperature environment to ignite the fuel once it is injected. In an HCCI engine the fuel is injected much earlier, very often during the intake stroke or early compression stroke to generate a more homogeneous fuel-lean mixture. In PPC engines, the injection timing of the fuel is in-between that of HCCI and Diesel engines.

17.4.1 Numerical Simulation of HCCI Engines

HCCI engine has been developed since the 1980s (Najt and Foster 1983; Onishi et al. 1979; Thring 1989). In HCCI engines, the fuel and air are premixed or nearly premixed since in direct injection HCCI engines the mixture will unavoidably have stratification in both composition and temperature. Nevertheless, the local mixture is under the fuel-lean condition and sometimes exhaust gas recirculation (EGR) is used to dilute the fuel/air mixture. The combustion temperature is therefore low, which results in low NO_x emissions. The fuel-lean mixture is advantageous for suppression of soot formation in compression ignition engines. HCCI engines have higher engine efficiency than SI engines due to its higher compression ratio, and have lower soot and NO_x emissions than Diesel engines due to the premixed fuel-lean mixture. A comprehensive review on HCCI engines has been given by Yao et al. (2009).

17.4.1.1 DNS of HCCI Combustion Process

An ideal HCCI with homogeneous composition and temperature in the engine cylinder would have a homogeneous ignition and the process would be dictated by the chemical kinetics. In practical HCCI engines, the composition and temperature are stratified and engine experiments have indicated the existence of distinct reaction fronts (Christensen et al. 1999). These reaction fronts propagate at a speed typically an order of magnitude higher than that found in SI engines. DNS of generic HCCI combustion processes has been carried out aiming at understanding the reaction zone structures, the propagation velocity of the reaction fronts, and factors that govern the pressure-rise rate and heat release rates, etc., under HCCI engine relevant conditions.

In a two-dimensional DNS (2D-DNS) study, Sankaran et al. (2005) studied the effect of the stratification of initial temperature fields on the initial ignition and subsequent heat release of lean fully premixed H_2 /air ignition, and they found that both spontaneous ignition reaction fronts and premixed flame fronts can exist in the domain. Spontaneous ignition is dominant in the initial start of ignition, followed by a mixed mode of spontaneous ignition and premixed flame propagation, and in the end the remaining mixture is combusted in the mode of spontaneous ignition. The conclusion has been confirmed in other 2D-DNS (Chen et al. 2006; Zhang et al. 2016) and three-dimensional DNS (3D-DNS) (Yu and Bai 2013). In a recent 2D-DNS study of H_2 /air HCCI combustion with both stratified composition and temperature, as well as different intensities of turbulence, Zhang et al. (2016) reported that the heat release rate profile in the HCCI cases shows an apparently slower rate of overall heat release than that in the corresponding ideal HCCI case (without any stratification). It further shows that higher turbulence intensity yields a retarded autoignition and a shorter combustion duration. A larger composition stratification leads to an earlier onset of ignition and prolonged combustion duration. The statistics of local displacement speed of the reaction front shows the peak of the local displacement velocity decreases as the combustion proceeds.

Figure 17.1 shows the temperature distribution in the H_2 /air mixture under conditions similar to that of Zhang et al. (2016), with both composition and initial temperature stratification, but at a higher initial pressure. Due to the composition and temperature stratification the ignition of the mixture is nonhomogeneous in space. The reaction fronts (as indicated by the fronts of the high temperature zones) are strongly affected by turbulent eddies. At low turbulent rms velocity ($u'_{rms} = 0.2m/s$) the reaction fronts are more of circular shape whereas at a higher turbulent rms velocity ($u'_{rms} = 2m/s$) they are highly distorted by the turbulence eddies. Turbulence is shown to prolong the ignition delay time and shorten the combustion duration (Yoo et al. 2011; Zhang et al. 2016), which is not primarily due to the direct interaction of turbulence eddies with the reaction fronts, but mainly owing to the effect of turbulence on the temperature field prior to the onset of ignition. With strong turbulence the composition and temperature stratification are reduced by eddy mixing. The local temperature maximum is therefore reduced, which results in a retarded ignition. A lower degree of thermal and composition stratification implies a faster propagation velocity of the reaction front, thereby, a shorter combustion duration.

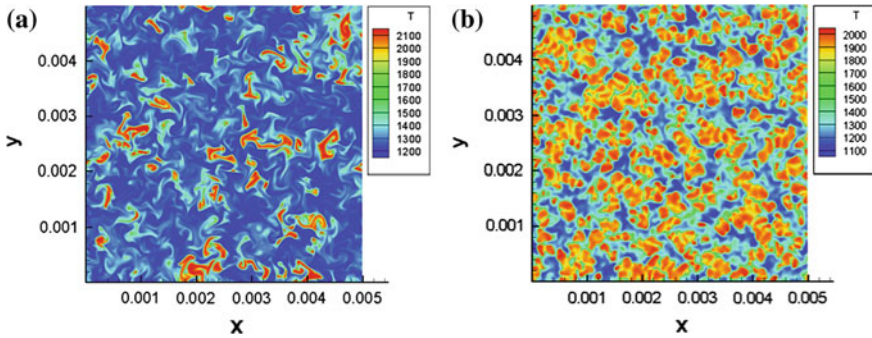


Fig. 17.1 Temperature distribution during the ignition stage in a H_2 /air mixture with two different turbulent velocities, **a** $u'_{rms} = 0.2m/s$, **b** $u'_{rms} = 2m/s$. The initial temperature is 1175K with a temperature fluctuation of $\pm 15K$, the mean equivalence ratio is 0.67, with an equivalence ratio stratification of ± 0.05 , the initial pressure is 118 bar. The domain has a dimension of 5×5 mm

Chen et al. (2006) developed a numerical diagnostics approach for analysis of the reaction front propagation in HCCI combustion. An indicator of front propagation due to deflagration or spontaneous ignition was proposed based on the local front displacement speed. The diagnostic approach was applied in studies of the effect of the initial temperature and turbulence field on HCCI combustion (Hawkes et al. 2006), and the effect of differential diffusion during auto-ignition of a hydrogen/air mixture (Bisetti et al. 2009).

The reaction front propagation in HCCI combustion is further studied in a H_2 /air mixture in both two-dimensional and three-dimensionality configurations (Yu and Bai 2013). Compared with 2D-DNS, 3D-DNS predicted a delayed but more rapid heat release rate (15% higher in peak value). The difference is due to that, compared with 2D turbulence, 3D turbulence yields a faster heat transfer rate that leads to a more homogenous temperature field prior to the onset of ignition. The faster heat transfer rate in the 3D case is a consequence of one extra spatial dimension, which gives rise to both a higher value of initial velocity strain rate and an additional strain-self-amplification, which then leads to a faster production of temperature gradient and quicker mixing of the temperature field. It was also found that the higher 3D peak heat release rate is mainly due to the larger reaction front area in 3D-DNS, while the mean propagation speed of reaction fronts is similar in 3D and 2D.

17.4.1.2 Modeling of HCCI Combustion Process

The DNS results discussed in Sect. 17.4.1.1 indicate the co-existence of premixed flame fronts and spontaneous ignition fronts in HCCI combustion. The specialized models developed for the modeling of turbulent premixed flames in SI engines are generally not useful in modeling of HCCI engines. The paramount importance of chemical kinetics in HCCI combustion demands the use of finite-rate chemistry

models in simulation of HCCI combustion. The strong effect of turbulence mixing on the HCCI combustion process, especially on the composition and thermal stratification prior to the onset of ignition, requires a decent modeling of the turbulent mixing process, e.g., the modeling of the turbulent transport fluxes in Eq. (17.3). Although the HCCI reaction fronts are very thin, cf. Fig. 5 in Zhang et al. (2016), considerably thinner than the mesh size used in RANS and LES, it may, however, be not necessary to consider these thin reaction zone structures in the modeling of the mean reaction rate in RANS or the filtered reaction rate in LES, i.e., $\tilde{\omega}_k$ in Eq. (17.3). This is owing to that the prediction of the reaction front propagation depends mainly on the prediction of the onset of ignition, which depends on the temperature and composition field prior to the onset of ignition. These fields are much smoother than those after the onset of ignition. In practice, a simple PaSR model or WSR model is sufficient in modeling the $\tilde{\omega}_k$ term in RANS and LES. Furthermore, the relatively low ratio of the magnitude of diffusive transport terms to that of the reaction rates, cf. Chen et al. (2006) and Yu and Bhai (2013), implies that the unresolved gradient of composition or temperature across the thin reaction zone does not affect the propagation of the reaction fronts to an appreciate level.

A large number of HCCI engine simulations have been carried out using the so-called multi-zone model (Aceves et al. 2000; Babajimopoulos et al. 2015; Flowers et al. 2003), in which detailed chemical kinetic mechanisms are integrated in a small number of temperature zones. This type model has shown a low-computational cost and reasonably accurate prediction of HCCI engine combustion. More details about the multi-zone model will be given in Sect. 17.5.1.

Another type of HCCI engine combustion simulation is based on the tabulation approaches to couple the ignition chemistry in CFD simulations (Joelsson et al. 2012; Knop et al. 2011; Lecocq et al. 2011; Yu et al. 2006, 2007). In these models, the mean source term in Eq. (17.6) is computed through lookup tables based on the ignition calculation in homogenous mixture with detailed chemical kinetic mechanisms. An example of application of the tabulation approach to LES of HCCI engine combustion can be found in Yu et al. (2007).

17.4.2 Numerical Simulation of PPC Engines

The challenge in HCCI engine is its high sensitivity to engine operation conditions. The combustion process is highly sensitive to the temperature of the charge; at light load operation, unburned fuel, and CO emissions are cumbersome, and it is also difficult to ignite the mixture in cold-start. At heavy load the combustion heat release rate is high, which can give rise to high engine noise. To circumvent some of these drawbacks, other types of LTC combustion concepts have been developed for ICE. One of these is the concept of the partially premixed combustion (PPC) engine. PPC engine is a hybrid of the conventional Diesel engine (CDE) and HCCI engine. In PPC engines, the fuel is injected much earlier than that in Diesel engines but later than that in HCCI engines. Unlike CDE, in PPC engines there is a sufficiently long

time separation between the end of injection and the onset of autoignition, so that the fuel can sufficiently mix with the air. Unlike HCCI engines, the fuel stratification is large in PPC engines so that a slower heat release rate can be obtained.

Kalghatgi et al. (2007) showed that with highly reactive fuels such as diesel, a large amount of exhaust gas recirculation (EGR) or low compression ratio is needed to separate the end of the fuel injection and the start of combustion, and thus, high octane number fuel was suggested. Manente et al. (2009) examined the performance of a PPC engine with gasoline fuel and a rather high pressure-rise rate with a reduced engine efficiency was noticed. A way to ensure a desirable mixture for PPC is to split the fuel injection into different times. Hanson et al. (2009) investigated a heavy duty PPC engine with two injections of gasoline. They examined the effect of the fuel split between the first and the second injections and found that there was a tradeoff between emissions of NO_x and soot, i.e., the reduction of NO_x was accompanied by the increase of soot emission. Manente et al. (2010) investigated the use of ethanol as the fuel in PPC engines, and they found that the best engine performance could be achieved with the mass ratio of the fuel through the first injection and the second injection about 1. Although PPC engine showed a great potential in achieving a better tradeoff between engine efficiency and emissions the control of the fuel injection is not a trivial task. The combustion physics in PPC engines is relatively less understood; numerical simulations can play an important role in developing PPC engines.

17.4.2.1 DNS of PPC Engine Combustion Process

Zhang et al. (2015a, b) carried out DNS studies of PPC in a mixture of primary reference fuel (PRF70, with 70% iso-octane and 30% n-heptane on volume basis), air and EGR in a constant volume domain, under conditions relevant to PPC engines with two injections. The first injection of the fuel was assumed to mix with the air and EGR perfectly (representing the case of an early injection of the fuel in PPC engines), and the second injection was assumed to start later in the compression stroke (near TDC). The DNS results revealed the fundamental combustion process and the reaction zone structure in the PPC mixture of PRF70, air and EGR.

Figure 17.2 shows the reaction zone structures depicted by key species and the heat release rate at two points in time. A sequential combustion process is identified from the DNS results, which is the reason behind the slower heat release rate and the tradeoff between NO_x emission and CO emission. The combustion process starts with the ignition of the mixture. The ignition process of the mixture in the fuel-lean region (where the fuel is from the first injection) converts the fuel to CO, which is subsequently oxidized to CO₂. This is similar to the HCCI combustion process. In this process, the heat release is typically rapid; the peak heat release rate depends on the homogeneity of the composition and temperature, as well as the equivalence ratio of the mixture. The latter can be controlled by the amount of fuel in the first injection. The ignition process of the fuel-rich mixtures (the fuel is mainly from the second injection) converts the fuel to combustion intermediates (mainly CO and H₂), which can not be oxidized further without mixing with the oxidiser in the fuel-lean

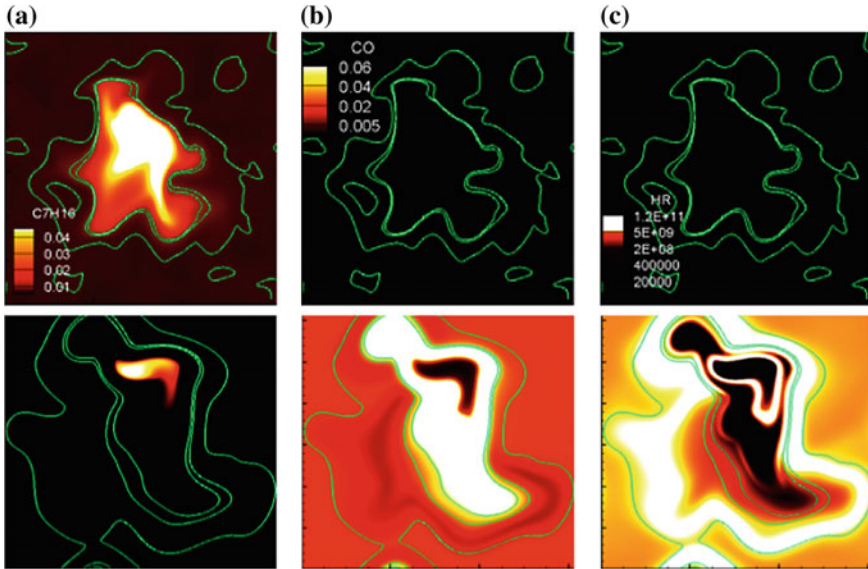


Fig. 17.2 Distributions of heat release rate (HR) and mass fractions of n-heptane and CO in a mixture of PRF70, air and EGR at two instances of time during PPC combustion process; **a** mass fraction of n-heptane, **b** mass fraction of CO, **c** heat release rate. Upper row: at 0.0317 ms; lower row: at 0.2 ms. The iso-lines correspond to the local equivalence ratio of 1.2 (the innermost line), 1 (the middle line), and 0.5 (the outermost line). The domain has a dimension of 0.614 mm \times 0.614 mm. More details about the DNS results can be found in Zhang et al. (2015a, b)

region. Thus, the oxidation of the intermediate products in the fuel-rich region is in a diffusion flame mode, which is governed by turbulence mixing, and is typically much slower than that of the ignition process of HCCI.

Three distinctive regions are identified in PPC combustion (Zhang et al. 2012, 2015a, b), a lean nearly homogeneous charge region, a stoichiometric charge region and a fuel-rich charge region. NO formation is mainly during the combustion in the stoichiometric charge region due to the high combustion temperature. This implies that the interface between the first injection and the second injection should be decreased to reduce the NO emissions. The CO emission is mainly from the fuel-rich charge region where CO formed in the fuel-rich mixture undergoes oxidation reactions in the later stage of combustion, which is at the diffusion flame mode and dictated by the turbulence mixing process. The emission of CO increases with the mass of the fuel in the second injection.

Turbulence has a more important impact on PPC process than on the HCCI process. Similar to the HCCI process, increase in turbulence intensity leads to a rather significant increase in the peak heat release rate, owing to the faster mixing between the fuel-rich pocket and the fuel-lean mixture, which leads to more homogeneous mixture in the domain, thereby, a more rapid combustion process once it is started. Furthermore, with larger turbulence integral length or higher turbulence

intensity, thus a higher mixing rate, the CO oxidation process is enhanced and the emission of CO is reduced, however, at a cost of higher NO emission due to more complete combustion and thus higher temperature (Zhang et al. 2015b).

17.4.2.2 Modeling of PPC Engine Combustion Process

DNS results reported in Zhang et al. (2012, 2015a, b) indicate that the combustion process in PPC engines is at multiple modes. In the first stage, the combustion process is similar to that of HCCI, where the dominant mode is spontaneous autoignition of the mixture. Models developed for HCCI can be used to simulate the ignition process in PPC engines. The later stage of the PPC process is at the diffusion flame mode. Models developed for Diesel engine combustion are therefore usable for this stage of combustion. By coupling a multi-zone type of model and a flamelet type of model one can expect that a highly efficient, specialized model for PPC engines can be developed. This type of model is however complex to implement into CFD codes, and it is rarely reported in the literature.

Numerical simulations of PPC combustion has been carried out using a more general type of models, e.g., finite-rate chemistry (FRC) models. Solsjo et al. (2012) applied a FRC model based on the WSR to LES study of the mixing, ignition, and combustion processes in a laboratory engine operating under PPC conditions. It was shown that the model could capture the main features of PPC engine under conditions of different swirl numbers and injections. Jangi et al. (2017) compared two FRC models in RANS simulations of a methanol fuelled compression ignition engine that operated under both HCCI and PPC conditions. One was based on the Eulerian stochastic fields (ESF) PDF model and the other based on the WSR model. It was shown that the two model yielded similar results for the HCCI case with an earlier injection of methanol, whereas for the PPC case with later methanol injection the PDF model predicted an in-cylinder pressure profile in good agreement with the experiments, while the WSR model predicted a much slow ignition. In RANS simulation, the temperature field is smoothed, thus, the hot spot in the mixture prior to ignition is cooled, which results in a delayed onset of ignition with a WSR model. In PDF models, certain temperature fluctuations are incorporated into the simulations through the stochastic process, which leads to an earlier onset ignition. The LES-based WSR model allows for more realistic spatial variations of temperature and composition; thus, LES-WSR could predict more physical results in PPC engine simulations.

17.4.3 Numerical Simulation of RCCI Engines

Reactivity controlled compression ignition (RCCI) (Kokjohn et al. 2011; Reitz and Ganesh 2015) is another novel concept that can be used to circumvent the problems of control of HCCI ignition timing and heat release rate. In RCCI, a low reactivity

fuel (e.g., gasoline) is injected to the intake port together with the air supply and a homogeneous mixture of the low reactivity fuel and air is formed in the cylinder before the injection of a high reactivity fuel (e.g., diesel) to initiate the ignition. The ignition timing is therefore controlled by the injection of the high reactivity fuel, while the heat release rate is controlled by the mass split of the two fuels. The RCCI concept is very attractive for the application of alternative fuels in ICE. Natural gas and alcohols are examples of the attractive alternative fuels. These fuels have high octane numbers and they are difficult to use in compression ignition engines. One can improve the ignition property of these fuels by injecting another fuel (e.g., diesel) that is easy to ignite to initiate the ignition of high octane number fuels.

A number of investigations have been conducted on methanol/diesel RCCI engines to study its emission characteristics, e.g., Dempsey et al. (2013); Li et al. (2014); Masimalai (2014); Yao et al. (2008). With increasing methanol/diesel mass ratio the emission of soot and NO_x was shown to decrease; however, the emission of unburned hydrocarbons and CO could increase due to the decreased combustion efficiency and increased fuel/air ratio in the methanol/air mixture (Masimalai 2014). It has been observed that the overall engine performance and emissions are rather sensitive to the intake temperature and the amount of EGR, due to their influence on the in-cylinder gas temperature prior to the onset of ignition. A high initial temperature in the methanol/air/EGR mixture could give rise to fast ignition in the methanol/air/EGR mixture in a way similar to HCCI engines, with rather high heat release rate and pressure-rise rate. A low initial temperature could delay the ignition of the high reactivity fuel, which can allow for more complete mixing of the high reactivity fuel with methanol/air/EGR before the onset of ignition, thus resulting in a rather different heat release profile (Hu et al. 2017). At low load and cold start, this could give rise to misfire (Yao et al. 2008). Some experimental studies have shown rather high pressure-rise rate and noise level of this type of dual fuel combustion at high methanol/diesel ratio, which could limit the amount of methanol to be used to substitute diesel in the engine (Popa et al. 2001).

17.4.3.1 DNS of RCCI Combustion Process

Hu et al. (2017) carried out two-dimensional and three-dimensional DNS studies of RCCI combustion with methanol and n-heptane as fuels in a constant volume domain with a dimensional of 14×12 mm (2D-DNS) and $14 \times 12 \times 2$ mm (3D-DNS). For the initial condition, methanol was assumed to have perfectly mixed with air and EGR, and the initial pressure was set to 42 bar. The EGR/air molar ratio was 1:1. The equivalence ratio of methanol/air/EGR mixture was 0.6. Gaseous n-heptane/air mixture was then injected, which initiated the ignition of the mixture. It was shown that the RCCI combustion can occur at different modes. The ignition of the mixture is at the mixing layer of the n-heptane jet; thereafter, the combustion process in the ambient methanol/air/EGR mixture can be at spontaneous ignition mode or premixed flame propagation mode. Finally, the combustion intermediate from the incomplete

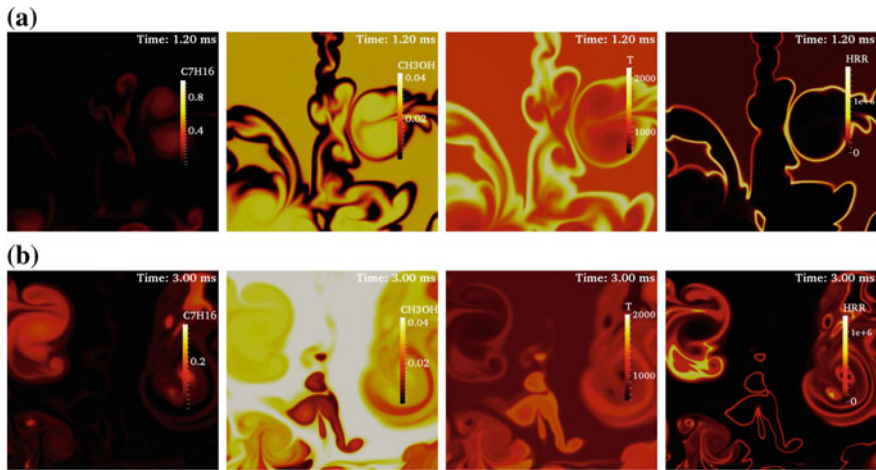


Fig. 17.3 Distributions of mass fractions of n-heptane (C7H16) and methanol (CH3OH), local temperature (T), and local heat release rate (HRR) during the combustion process of n-heptane, methanol, air, and EGR in a constant volume domain under conditions relevant to RCCI engines; **a** Initial temperature of 1000 K, **b** Initial temperature of 800 K. The initial pressure is 42 bar. The domain has a dimension of 14×12 mm. More details about the DNS results can be found in Hu et al. (2017)

oxidation of n-heptane can be burned in diffusion flame mode, by mixing with the remaining oxidizer in the ambient mixture.

Figure 17.3 shows the mass fractions of n-heptane and methanol, as well as local temperature and local heat release rate in the domain under two different initial temperature conditions, at the instance of time of peak overall heat release rate of the domain. At the initial temperature of 1000 K, the ignition occurs rather quickly, with the maximal heat release rate occurring at 1.2 ms. The highest temperature and the highest local heat release rate are found in the mixing layer between the n-heptane jet and the ambient mixture. In the ambient methanol/air/EGR mixture, the temperature and local heat release rate are also rather high, indicating that the mixture is undergoing autoignition, a process similar to that in HCCI engines. Due to the autoignition of the entire ambient mixture the peak overall heat release rate is rather high. The combustion mode in the low-initial temperature case (with initial temperature of 800 K) is different. The mixture ignites much later, which allows for a better mixing of n-heptane and the ambient methanol/air/EGR mixture. Due to the low-initial temperature, the ambient methanol/air/EGR mixture is combusted at a premixed flame mode.

Turbulence has an important effect on the RCCI process, in a way similar to that on the PPC process. Turbulence has an indirect effect on the ignition of the fuel/air mixture—by affecting the temperature and mixture fields prior to the onset of ignition. Turbulence has a more important impact on the later stage diffusion controlled combustion process, by controlling the mixing rate of the combustion intermediates

in the fuel-rich region with the oxygen in the fuel-lean region. Under low-initial temperature conditions, turbulence can directly affect the propagation of the premixed flame by wrinkling the flame front.

17.4.3.2 Modeling of RCCI Engine Combustion

Due to the existence of multiple modes in RCCI engine combustion, general models based on the finite-rate chemistry have been used in practical RCCI engine simulations, cf. Dempsey et al. 2013; Li et al. 2014. Li et al. (2014) used a KIVA 3V RANS code, where finite-rate chemistry was coupled with flow simulation using Chemkin solver to perform an optimization study of methanol/diesel RCCI engines. The mean reaction rate $\tilde{\omega}_k$ was modeled using the WSR model. This model has been used in HCCI and PPC engines simulations as discussed earlier. The results were shown to agree reasonably well with the engine in-cylinder pressure measurements and global heat release rate data. Such model is adequate for capturing the ignition process of RCCI, owing to the low sensitivity of the results to grid resolution. However, it is expected that the model is not accurate for simulation of the premixed flame propagation stage of RCCI combustion, which may occur at light load conditions. The model is also computationally demanding due to the direct solution of the species transport equations, especially when the chemical kinetic mechanism is large.

17.5 Speedup of Numerical Simulation Based on the Finite-Rate Chemistry

Combustion in ICE often involves multiple combustion modes, e.g., in SI engines turbulent premixed flames with possible autoignition, in Diesel engines starting with the onset of autoignition, ignition assisted premixed flame propagation at the leading front of the spray flame, and diffusion flames in the main part of the spray flame. In modern LTC engines, e.g., HCCI, PPC, and RCCI, spontaneous ignition and premixed flame propagation are frequently observed, and in the later stage of PPC and RCCI combustion, the process is at the diffusion controlled flame mode in which combustion intermediates such as CO and H₂ from the incomplete oxidation of the fuel in the fuel-rich region of the mixture is further continued. In most numerical simulations reported in the literature, finite-rate chemistry, FRC, coupling with the flow transport simulations has been frequently used. FRC has shown reasonable success in simulation of multiple mode combustion processes, especially in compression ignition engines. One main challenge in FRC models is the long computational time required due to the solution of a large number of species transport equations, specially due to the stiffness of the chemistry. Different approaches have been developed for efficiently coupling the chemistry with flow simulations, e.g., the computational singularity perturbation (CSP) approach (Lam and Goussis 1988), the intrinsic low-

dimension manifold (ILDM) approach (Maas and Pope 1992), the in situ adaptive tabulation (ISAT) (Pope 1997) approach, the direct relation graph (DRG) approach (Lu and Law 2005), and the dynamic adaptive chemistry (DAC) approach (Liang et al. 2009), among others. Details about these methods can be found in the above cited papers and references therein. In the remainder of this section, we will focus on two methods that are easy to implement and efficient in speeding up FRC simulations. The first is the multi-zone approach for HCCI engine simulations (Aceves et al. 2000) and the second is the chemistry coordinate mapping approach for multi-mode LTC engine simulations (Jangi and Bai 2012; Jangi et al. 2011).

17.5.1 Multi-zone Model

As discussed in Sect. 17.4.1.1 in HCCI the dominant process is the spontaneous ignition, although one can also find premixed flame propagation in the intermediate stage of HCCI combustion. When the ignition is the main process, in the transport equations for species mass fractions, the diffusive transport term is smaller than the chemical reaction rates. The chemical reaction rates depend on the local thermodynamic properties such as species mass fractions and temperature. In HCCI engines, if the composition stratification is small, the ignition process is dictated by the thermal stratification inside the cylinder.

The multi-zone model is based on the assumption that the HCCI combustion process depends only on the local temperature. In an engine cylinder with a stratified temperature field, the combustion process in different spatial locations in the cylinder would be the same if the temperature in these locations were the same. Based on this argument, one does not need to integrate the chemical reaction rates in each CFD cell in the cylinder but rather integrate the reaction rates for a number of different temperatures. The species and temperature evolutions in each temperature zone will be the same in the CFD cells that share the same temperature as that in the temperature zone.

Aceves et al. (2000) presented a multi-zone simulation of an HCCI engine. First, the KIVA code was run to simulate the temperature distribution inside the cylinder without combustion, based on which a number of temperature zones was selected. In each of the temperature zones, the evolutions of species and temperature were simulated using a detailed chemical kinetics code as the multi-zone solver (the HCT code; Hydrodynamics, Chemistry, and Transport). In each temperature zone the mass was conserved during the multi-zone ignition simulation, while the pressure in all temperature zones was kept the same. The volume of each temperature zone was therefore varied during ignition simulations. With only 10 temperature zones the predicted in-cylinder pressure evolution was already in satisfactory agreement with the experiments. The CO prediction is, however, less accurate. In practical engines, CO was typically not consumed completely in the lowest temperature regions of the combustion chamber. It diffuses back into the hotter gasses in the core of the combustion

chamber, where it is further oxidized. Thus, mixing of mass between the temperature zones should be taken into account in the prediction of the composition field.

The limitation of the original multi-zone method is that once the chemistry calculation begins, the detailed information from the CFD code is lost and there is no mixing between the zones. This is due to that the neighboring temperature zones are physically not always neighbors in space. The temperature zones interact one another only through the adjustment of pressure. Flowers et al. (2003) modified the multi-zone model to include the mixing effects, by introducing a coupled CFD/multi-zone model. Instead of a one-way mapping of the CFD temperature distribution onto the multi-zone chemical kinetics solver, their method proposed a two-way mapping of information back and forth throughout the cycle. In the coupled CFD/multi-zone model, one CFD time step is split into chemistry fractional steps and flow convection and diffusion fractional time steps. The chemistry solver is used in the temperature zones (the number of temperature zones is much fewer than the CFD cells) to integrate the chemical reaction source terms in the species transport equations, to obtain a fractional change of species composition. The new species composition after the chemistry fractional step is then mapped back to the CFD cells. Thereafter, integration of the convection and diffusion terms is carried out in the CFD cells to complete the time step. Flowers et al. (2003) showed that, with mixing taken into account the prediction of CO was significantly improved.

Babajimopoulos et al. (2015) extended the coupled multi-zone model to HCCI engine simulation with stratification in both temperature and compositions. The multi-zones are extended into two-dimensional phase space, with temperature and a progress equivalence ratio as the coordinates. The proposed methodology showed a reduction of 90% of the computational time, while maintaining good agreement with the detailed solution.

Goldin et al. (2009) presented a cell agglomeration (CA) algorithm to speedup the numerical simulations coupled with detailed chemistry. Similar to the extended multi-zone model (Babajimopoulos et al. 2015; Flowers et al. 2003), the CA method is based on the fractional time-step integration of the flow transport terms and the chemical reaction rates. In the CA algorithm, the integration of the chemical reaction rates is done in the space of composition (N_s -dimension, N_s is the number of species in the mixture), temperature, and pressure. A uniform Cartesian mesh, in composition space was used to group computational cells with similar thermochemical composition, temperature and pressure at every reaction sub-time step. The new composition was mapped back to the CFD cells where the integration of the flow transport terms was carried out to complete the integration of one CFD time step. While the CA method is more general than the earlier multi-zone models, the large dimension of composition space is the challenge. Goldin et al. (2009) demonstrated the use of a subset of the composition space, e.g., with 11 dimensions (including T , N_2 , O_2 , CH_4 , CO_2 , H_2O , CO , OH , H_2 , O and CH_2O) for two-dimensional methane/air premixed flame simulation, and a factor of three speedup rate of the simulations was achieved.

17.5.2 Multi-zone Chemistry Coordinate Mapping Method

Similar to that of the multi-zone model and the cell agglomeration method, the multi-zone chemistry coordinate mapping (CCM) approach is based also on the fractional step CFD method, in which the integration of the different terms of the governing equations within a CFD time step is split into several fractional time steps. In RANS and LES, even in DNS (Yu et al. 2012), the CFD time step determined by the CFL number is too large for the integration of the chemical reaction rates, due to the large span of time scales of chemistry. Thus, multiple small fractional sub-time steps are used within each CFD time step to integrate the stiff chemistry.

The time-consuming part of the numerical simulation is the integration of the chemical reaction rates. As shown earlier, the integration of chemical reaction rates can be done in low-dimension chemistry zones. Each zone corresponds to a number of different CFD cells in the physical domain, so integration of the chemical reaction rates and heat release rate is not performed in every CFD cell in the physical domain. The results in the chemistry zones are mapped back to the CFD cells in physical domain, and subsequently integrated to the flow transport terms in every CFD cell in the physical domain. This procedure decreases the computational cost significantly since it is possible to group physical cells into a much smaller number of chemistry zones.

It is clear that the key issue of this approach is the selection of the chemical phase space. The extended multi-zone model of Flower et al. (2003) used temperature as the phase space coordinate; the model of Babajimopoulos et al. (2015) used temperature and a progress equivalence ratio, while the CA algorithm of Goldin et al. (2009) used temperature and the mass fractions of a number of key species. In a series of DNS studies of H_2 /air HCCI combustion, methane/air premixed flames, and CO/H_2 /air premixed flames under constant volume conditions (all cases with initial homogeneous composition fields, relevant to conditions in HCCI and SI engines), Jangi et al. (2011) proposed a two-dimensional phase space, with the element mass fraction of H and temperature as the phase space coordinates. Temperature was used to characterize the reaction progress, whereas the H element mass fraction to characterize the differential diffusion effect in an initially premixed mixture. The method was referred to as the multi-zone chemistry coordinate mapping (CCM), since it involved a two-way mapping between the CFD cells in physical domain and the multi-zone cells in the chemistry phase space. The 2D DNS with CCM was shown to reduce the DNS CPU time by nearly 70% with nearly the same results as that obtained from the full DNS. For 3D simulations the speedup is much greater.

The CCM and its associated errors were evaluated in a DNS of autoignition of an n-heptane jet discharged into a hot atmosphere, and in a RANS of spray combustion in a constant volume combustion vessel (Jangi and Bai 2012). It was shown that a four-dimensional phase space, with temperature, mass fraction of H element, mass fraction of the fuel (n-heptane), and scalar dissipation rate of the element mass fraction of H as the phase space coordinates predicted satisfactory results. The CCM approach was shown to be suitable for numerical simulations of liquid n-heptane

spray combustion based on the RANS models. The transient processes of spray mixing with the ambient air, ignition of the mixture, and stabilization of the mixing controlled diffusion flames were well predicted by the RANS-CCM model. RANS-CCM replicated the same results as RANS with direct integration of the chemical reaction rates in the physical domain; the computational cost of RANS-CCM was, however, only 3–7% of that needed for RANS with the direct integration of chemistry.

The four-dimensional phase space was applied to study the effect of EGR on the structure and soot emissions in a diesel spray flame in a constant volume vessel (Jangi and Lucchini 2013), and the liftoff behavior of the spray flame of n-heptane in a Diesel engine (Solsjo et al. 2013), and the liftoff and flame structure of n-dodecane spray combustion in a constant volume combustion vessel (Gong et al. 2014). The results were promising in terms of accuracy and efficiency. Typically, a factor 30 speedup rate was achieved in these applications.

The CCM model was recently extended to couple with the particle-based transported PDF model that has the advantage to close the chemical reaction rates (Jangi et al. 2015). In this model, referred to as PDF-CCM, instead of identifying and clustering CFD cells into the CCM zones, the notional Lagrangian particles that were in similar thermodynamic states were identified and clustered into the phase-space zones. The method was applied to simulate methane/air lifted jet flames in vitiated coflow. The multiple modes combustion behavior at different ambient temperature conditions were well captured using PDF-CCM. Good agreement with experiments were observed while a speedup factor of 20 was reached in the simulations as compared with the original PDF model.

The PDF-CCM model has also been extended to the Eulerian stochastic field based PDF model (Jangi et al. 2015). The model is referred to as the ESF-CCM, in which the thermodynamic states of the discretized stochastic fields were mapped into a low-dimensional phase space. Integration of the chemical stiff ODEs was performed in the phase space and the results were mapped back to the physical domain. This method was shown to be able to speedup the original ESF-PDF model by a factor of 20 or more. The ESF-CCM model had shown good predictive potential in numerical simulation of various turbulent combustion processes, e.g., a lean pre-mixed flame blowoff process (Hodzic et al. 2017) and n-dodecane spray combustion in a constant volume combustion vessel (Gong et al. 2014).

17.6 Concluding Remarks

Numerical simulations are expected to play a more important role in designing future internal combustion engines that are facing increasingly stringent emission legislations and demands on engine efficiency. New engines are also required to run with alternative renewable fuels to achieve fossil-fuel-free transportation and sustainable development. While computers are becoming more powerful with time numerical simulations for design purpose will rely on combustion models that are not only robust, accurate but also efficient. Specialized models such as RIF, CFM and FGM

shall be developed further to simulate wider flame problems. General models such as those employing detailed chemistry will be used in the future for combustion processes that involves multiple combustion modes. Certainly, it is very important to develop chemical kinetic mechanisms that are on one hand accurate enough to describe the problem and on other hand of moderate size and stiffness, suitable for CFD simulations. To use these finite-rate chemistry-based models improving the computational efficiency is crucial. Methods, such as ISAT, ILDM, DRG, and DAC are expected to be important in practical applications, while methods based on the multi-zone/CCM concept shall be further developed. These models showed a promising speedup property. Further development of these models is needed to have a consistent and optimal phase space, in order to achieve a well-balanced accuracy and efficiency.

Acknowledgements The author acknowledges the financial support from the Swedish Energy Agency through KC-FP and CeCOST.

References

- Aceves SM, Flowers DL, Westbrook CK, Smith JR, Dibble RW, Christensen M, Pitz WJ, Johansson B (2000) A multi-zone model for prediction of HCCI combustion and emissions. SAE Technical Paper 2000-01-0327
- Babajimopoulos A, Assanis DN, Flowers DL, Aceves SM, Hessel RP (2015) A fully coupled computational fluid dynamics and multi-zone model with detailed chemical kinetics for the simulation of premixed charge compression ignition engines. *Int J Eng Res* 6:497–512
- Bisetti F, Chen JY, Chen JH, Hawkes ER (2009) Differential diffusion effects during the ignition of a thermally stratified premixed hydrogen-air mixture subject to turbulence. *Proc Combust Inst* 32:1465–1472
- Bray KNC, Libby PA, Moss JB (1985) Unified modeling approach for premixed turbulent combustion-part I: general formulation. *Combust Flame* 61:87–102
- Candel SM, Poinot TJ (1990) Flame stretch and the balance equation for the flame area. *Combust Sci Technol* 70:1–15
- Carlsson H, Nordström E, Bohlin A, Wu Y, Zhou B, Li ZS, Alden M, Bengtsson PE, Bai XS (2015) Numerical and experimental study of flame propagation and quenching of lean premixed turbulent low swirl flames at different Reynolds numbers. *Combust Flame* 162:2582–2591
- Chen JH (2011) Petascale direct numerical simulation of turbulent combustion-fundamental insights towards predictive models. *Proc Combust Inst* 33:99–123
- Chen JH, Hawkes ER, Sankaran R, Mason SD, Im HG (2006) Direct numerical simulation of ignition front propagation in a constant volume with temperature inhomogeneities: I. Fundamental analysis and diagnostics. *Combust Flame* 145:128–144
- Christensen M, Johansson B, Franke A, Richter M, Alden M (1999) A study of the homogeneous charge compression ignition combustion process by chemiluminescence imaging. SAE Technical Paper 1999-01-3680
- Colin O, Benkenida A (2004) The 3-Zones extended coherent flame model (ECFM3Z) for computing premixed/diffusion combustion. *Oil Gas Sci Technol Rev IFP* 59:593–609
- Colin O, Ducros F, Veynante D, Poinot T (2000) A thickened flame model for large eddy simulations of turbulent premixed combustion. *Phys Fluids* 12:1843
- De Paola G, Mastorakos E, Wright YM, Boulouchos K (2008) Diesel Engine Simulations with Multi-Dimensional Conditional Moment Closure. *Combust Sci Technol* 180:883–899

- Dec JE (1997) A conceptual model of DI diesel combustion based on laser-sheet imaging, SAE Technical Paper 970873
- Dempsey AB, Walker NR, Reitz R (2013) Effect of piston bowl geometry on dual fuel reactivity controlled compression ignition (RCCI) in a light-duty engine operated with gasoline/diesel and methanol/diesel. SAE Int J Eng 6:78–100
- D'Errico G, Lucchini T, Contino F, Jangi M, Bai XS (2014) Comparison of well-mixed and multiple representative interactive flamelet approaches for diesel spray combustion modelling. Combust Theor Modell 18:65–88
- Dunstan TD, Minamoto Y, Chakraborty N, Swaminathan N (2013) Scalar dissipation rate modelling for Large Eddy Simulation of turbulent premixed flames. Proc Combust Inst 34:1193–1201
- Felsch C, Luckhchoura V, Weber J, Peters N, Hasse C, Wiese W, Pischinger S, Kolbeck A, Adomeit P (2007) Applying representative interactive flamelets (RIF) with special emphasis on pollutant formation to simulate a DI diesel engine with roof-shaped combustion chamber and tumble charge motion, SAE Technical Paper 2007–01–0167
- Flowers D, Aceves S, Martinez-Frias J, Hessel R, Dibble R (2003) Effect of mixing on hydrocarbon and carbon monoxide emissions prediction for iso-octane HCCI engine combustion using a multi-zone detailed kinetics solver. SAE Technical Paper 2003–01–1821
- Ge HW, Shi Y, Reitz RD, Willems WW (2010) Engine development using multi-dimensional CFD and computer optimization, SAE Technical Paper 2010-01-0360
- Germano M, Piomelli U, Moin P, Cabot WH (1991) A dynamic subgrid-scale eddy viscosity model. Phys Fluids A: Fluid Dyn 3(7):1760–1765
- Goldin GM, Ren Z, Zahirovic S (2009) A cell agglomeration algorithm for accelerating detailed chemistry in CFD. Combust Theor Modell 13(4):721–739
- Gong C, Jangi M, Bai XS (2014) Large eddy simulation of n-Dodecane spray combustion in a high pressure combustion vessel. Appl Energy 136:373–381
- Hanson R, Splitter D, Reiz RD (2009) Operating a heavy-duty direct-injection compression-ignition engine with gasoline for low emissions. SAE Paper 2009-01-1442
- Hasse C, Barths H, Peters N (1999) Modelling the effect of split injections in diesel engines using representative interactive flamelets, SAE Technical Paper 1999–01–3547
- Hawkes ER, Sankaran R, Pebay PP, Chen JH (2006) Direct numerical simulation of ignition front propagation in a constant volume with temperature inhomogeneities II. Parametric study. Combust Flame 145:145–159
- Haworth DC (1999) Large-eddy simulation of in-cylinder flows, Oil & Gas Science and Technology-Rev. IFP 54:175–185
- Haworth DC (2010) Progress in probability density function methods for turbulent reacting flows. Prog Energy Combust Sci 36:168–259
- Heywood JB (1988) Internal combustion engine fundamentals. McGraw Hill Book Company, New York
- Hodzic E, Jangi M, Szasz RZ, Bai XS (2017) Large eddy simulation of bluff body flames close to blow-off using an Eulerian stochastic field method. Combust Flame 181:1–15
- Hu SY, Gong C, Bai XS (2017) Dual fuel combustion of n-heptane/methanol-air-EGR mixtures. Energy Procedia 105:4943–4948
- Jangi M, Bai XS (2012) Multidimensional chemistry coordinate mapping approach for combustion modelling with finite-rate chemistry. Combust Theor Model 16:1109–1132
- Jangi M, Yu R, Bai XS (2011) A multi-zone chemistry mapping approach for direct numerical simulation of auto-ignition and flame propagation in a constant volume enclosure. Combust Theor Model 16(2):221–249
- Jangi M, Zhao X, Haworth DC, Bai XS (2015) Stabilization and liftoff length of a non-premixed methane/air jet flame discharging into a high-temperature environment: An accelerated transported PDF method. Combust Flame 162(2):408–419
- Jangi M, Lucchini T, Gong C, Bai XS (2015) Effects of fuel cetane number on the structure of diesel spray combustion: An accelerated Eulerian stochastic fields method. Combust Theor Modell 19:549–567

- Jangi M, Li C, Shamun S, Tuner M, Bai XS (2017) Modelling of methanol combustion in a direct injection compression ignition engine using an accelerated stochastic fields method. *Energy Procedia* 105:1326–1331
- Jangi M, Lucchini TG, D'Errico, Bai XS (2013) Effects of EGR on the structure and emissions of diesel combustion. *Proc Combust Inst* 34:3091–3098
- Joelsson T, Yu R, Bai XS (2012) Large eddy simulation of turbulent combustion in a spark-assisted homogenous charge compression ignition engine. *Combust Sci Technol* 84:1051–1065
- Kalghatgi G, Risberg P, Angstrom H (2007) Partially pre-mixed auto-ignition of gasoline to attain low smoke and low NO_x at high load in a compression ignition engine and comparison with a diesel fuel. SAE Paper 2007-01-0006
- Klim WT, Huh KY (2002) Numerical simulation of spray autoignition by the first-order conditional moment closure model. *Proc Combust Inst* 29(2002):569–576
- Klimenko AY, Bilger RW (1999) Conditional moment closure for turbulent combustion. *Prog Energy Combust Sci* 25:595–687
- Knop V, Michel JB, Colin O (2011) On the use of a tabulation approach to model auto-ignition during flame propagation in SI engines. *Appl Energy* 88:4968–4979
- Kokjohn SL, Hanson RM, Splitter DA, Reitz RD (2011) Fuel reactivity controlled compression ignition (RCCI): a pathway to controlled high-efficiency clean combustion. *Int J Eng Res* 12:209–226
- Kong SC, Han Z, Reitz RD (1995) The development and application of a diesel ignition and combustion model for multidimensional engine simulation, SAE Technical paper 950278. <https://doi.org/10.4271/950278>
- Lam SH, Goussis DA (1988) Understanding complex chemical kinetics with computational singular perturbation. *Proc Combust Inst* 22:931–941
- Lecocq G, Richard S, Michel JB, Vervisch L (2011) A new LES model coupling flame surface density and tabulated kinetics approaches to investigate knock and pre-ignition in piston engines. *Proc Combust Inst* 33:3105–3114
- Li Y, Jia M, Hang Y, Liu Y, Xie M, Wang T et al (2014) Parametric study and optimization of a RCCI (reactivity controlled compression ignition) engine fueled with methanol and diesel. *Energy* 65:319–332
- Liang L, Stevens JG, Farrell JT (2009) A dynamic adaptive chemistry scheme for reactive flow computations. *Proc Combust Inst* 32:527–534
- Lu T, Law CK (2005) A directed relation graph method for mechanism reduction. *Proc Combust Inst* 30:1333–1341
- Maas U, Pope SB (1992) Simplifying chemical kinetics: intrinsic low-dimensional manifolds in composition space. *Combust Flame* 88:239–264
- Magnussen BF, Hjertager BH (1977) On mathematical modeling of turbulent combustion with special emphasis on soot formation and combustion. Symposium (International) on Combustion 16:719–729
- Manente V, Johansson B, Tunestal P (2010) Characterization of partially premixed combustion with ethanol: EGR sweeps, low and maximum loads. *J Eng Gas Turbines Power* 132:082802
- Manente V, Johansson B, Tunestal P (2009) Partially premixed combustion at high load using gasoline and ethanol, a comparison with diesel. SAE Technical Paper, 2009-01-0944
- Marble FE, Broadwell JE (1977) The coherent flame model for turbulent chemical reactions, Project Squid, Technical Report TRW-9-PU
- Martz JB, Kwak H, Im HG, Lavoie GA, Assanis DN (2011) Combustion regime of a reacting front propagating into an auto-igniting mixture. *Proc Combust Inst* 33:3001–3006
- Masimalai SK (2014) Influence of methanol induction on performance, emission and combustion behavior of a methanol–diesel dual fuel engine, SAE Technical Paper 2014-01-1315
- Mastorakos E, Bilger RW (1998) Second-order conditional moment closure for the autoignition of turbulent flows. *Phys Fluids* 10:1246
- Mittal V, Cook DJ, Pitsch H (2012) An extended multi-regime flamelet model for IC engines. *Combust Flame* 159:2767–2776

- Najt PM, Foster DE (1983) Compression ignited homogeneous charge combustion. SAE Technical paper 830264
- Nilsson P, Bai XS (2000) Level-set flamelet library approach for premixed turbulent combustion. *Experiment Thermal Fluid Sci* 21:87–98
- Nogenmyr KJ, Fureby C, Bai XS, Petersson P, Collin R, Linne M (2009) Large eddy simulation and laser diagnostic studies on a low swirl stratified premixed flame. *Combust Flame* 156:25–36
- Onishi S, Jo SH, Shoda K, Jo PD, Kato S (1979) Active thermo-atmosphere combustion—a new combustion process for internal combustion engines. SAE Technical paper 790501
- Pan J, Wei H, Shu G, Chen Z, Zhao P (2016) The role of low temperature chemistry in combustion mode development under elevated pressures. *Combust Flame* 174:179–193
- Persson H, Babajimopoulos A, Helmantel A, Holst F, Stenmark E (2017) Development of the combustion system for volvo cars Euro6d VEA diesel engine, SAE Technical Paper 2017-01-0713. <https://doi.org/10.4271/2017-01-0713>
- Peters N (2000) *Turbulent combustion*, Cambridge University Press
- Pitsch H, Barths H, Peters N (1996) Three-dimensional modeling of NOx and soot formation in DI-diesel engines using detailed chemistry based on the interactive flamelet approach, SAE Technical Paper 962057
- Popa MG, Megurescu N, Pana C, Racovitza A (2001) Results obtained by methanol fuelling diesel engine. SAE Technical Paper 2001-01-3748
- Pope SB (1985) Pdf methods for turbulent reactive flows. *Prog Energy Combust Sci* 11:119–192
- Pope SB (1988) The evolution of surfaces in turbulence. *Int J Eng Sci* 26:445–469
- Pope SB (1997) Computationally efficient implementation of combustion chemistry using in situ adaptive tabulation. *Combust Theor Modell* 1:41–63
- Reitz RD (1987) Modeling atomization processes in high-pressure vaporizing sprays. *Atomizat Spray Technol* 3:309–337
- Reitz RD, Ganesh D (2015) Review of high efficiency and clean reactivity controlled compression ignition (RCCI) combustion in internal combustion engines. *Prog Energy Combust Sci* 46:12–71
- Reitz RD, Rutland CJ (1995) Development and testing of diesel engine CFD models. *Prog Energy Combust Sci* 21:173–196
- Rutland CJ (2011) Large-eddy simulations for internal combustion engines—a review. *Int J Eng Res* 12:421–451
- Sankaran R, Im HG, Hawkes ER, Chen JH (2005) The effects of non-uniform temperature distribution on the ignition of a lean homogeneous hydrogen-air mixture. *Proc Combust Inst* 30:875–882
- Smagorinsky J (1963) General circulation experiments with the primitive equations: I. The basic equations. *Mon Weather Rev* 91:99–164
- Solsjo R, Jangi M, Chartier C, Andersson O, Bai XS (2013) Lift-off and stabilization of n-heptane combustion in a diesel engine with a multiple-nozzle injection. *Proc Combust Inst* 34:3031–3038
- Solsjo R, Jangi M, Tuner M, Bai XS (2012) Large eddy simulation of partially premixed combustion in an internal combustion engine. SAE Technical Paper 2012-01-0139
- Swaminathan N, Bilger RW (1999) Assessment of combustion submodels for turbulent non-premixed hydrocarbon flames. *Combust Flame* 116:519–545
- Tan Z, Reitz RD (2006) An ignition and combustion model based on the level-set method for spark ignition engine multidimensional modeling. *Combust Flame* 145:1–15
- Thring RH (1989) Homogeneous charge compression ignition (HCCI) engines. SAE Technical paper 892068
- van Oijen JA, Donini A, Bastiaans RJM, ten Thije Boonkkamp JHM, de Goey LPH (2016) State-of-the-art in premixed combustion modeling using flamelet generated manifolds. *Prog Energy Combust Sci* 57(2016):30–74
- Vermorel O, Richard S, Colin O, Angelberger C, Benkenida A, Veynante D (2009) Towards the understanding of cyclic variability in a spark ignited engine using multi-cycle LES. *Combust Flame* 156:1525–1541

- Yao C, Cheung CS, Cheng C, Wang Y, Chan TL, Lee SC (2008) Effect of diesel/methanol compound combustion on diesel engine combustion and emissions. *Energy Convers Manag* 49:1696–1704
- Yao M, Zheng Z, Liu H (2009) Progress and recent trends in homogeneous charge compression ignition (HCCI) engines. *Prog Energy Combust Sci* 35:398–437
- Yoo CS, Lu T, Chen JH, Law CK (2011) Direct numerical simulations of ignition of a lean n-heptane/air mixture with temperature inhomogeneities at constant volume: parametric study. *Combust Flame* 158:1727–1741
- Yu R, Bai XS (2013) Direct numerical simulation of lean hydrogen/air auto-ignition in a constant volume enclosure. *Combust Flame* 160:1706–1716
- Yu R, Yu J, Bai XS (2012) An improved high-order scheme for DNS of low Mach number turbulent reacting flows based on stiff chemistry solver. *J Comput Phys* 231:5504–5521
- Yu R, Bai XS, Lehtiniemi H, Ahmed SS, Mauss F, Richter M, Alden M, Hildingsson L, Johansson B, Hultqvist A (2006) Effect of turbulence and initial temperature inhomogeneity on homogeneous charge compression ignition combustion. SAE Technical Paper, 2006-01-3318
- Yu R, Bai XS, Vressner A, Hultqvist A, Johansson B, Olofsson J, Seyfried H, Sjöholm JO, Richter M, Alden M (2007) Effect of turbulence on HCCI combustion. SAE Technical Paper, 2007-01-0183
- Zeldovich YB (1980) Regime classification of an exothermic reaction with nonuniform initial conditions. *Combust Flame* 39:211–214
- Zhang F, Yu R, Bai XS (2012) Detailed numerical simulation of syngas combustion under partially premixed combustion engine conditions. *Int J Hydro Energy* 37:17285–17293
- Zhang F, Liu HF, Yu R, Yao M, Bai XS (2016) Direct numerical simulation of H₂/air combustion with composition stratification in a constant volume enclosure relevant to HCCI engines. *Int J Hydrog Energy* 41:13758–13770
- Zhang F, Yu R, Bai XS (2015a) Direct numerical simulation of PRF70/air partially premixed combustion under IC engine conditions. *Proc Combust Inst* 35:2975–2982
- Zhang F, Yu R, Bai XS (2015b) Effect of split fuel injection on heat release and pollutant emissions in partially premixed combustion of PRF70/air/EGR mixtures. *Appl Energy* 149:283–296